TECHNICAL MEMORANDUM

448

Experimental use of TRMM Precipitation Radar observations in 1D+4D–Var assimilation

Angela Benedetti, Philippe Lopez, Peter Bauer and Emmanuel Moreau

Research Department

Submitted to *Quarterly Journal of the Royal Meteorological Society*

August 2004

European Centre for Medium-Range Weather Forecasts
Europäisches Zentrum für mittelfristige Wettervorhersage
Centre européen pour les prévisions météorologiques à moyen terme

Series: ECMWF Technical Memoranda

A full list of ECMWF Publications can be found on our web site under:
http://www.ecmwf.int/publications/

Contact: library@ecmwf.int

European Centre for Medium-Range Weather Forecasts
Shinfield Park, Reading, RG2 9AX, England

Abstract

This paper presents a new application of the Tropical Rainfall Measuring Mission (TRMM) Precipitation Radar (PR) observations for indirect four–dimensional assimilation into the European Centre Medium–Range Weather Forecast (ECMWF) model. The PR reflectivities are first processed using a one–dimensional variational (1D–Var) method to adjust model temperature and specific humidity. The Total Column Water Vapour is then calculated via vertical integration of the humidity profile and assimilated into the operational four–dimensional variational (4D–Var) system.

Several case studies were run to assess the feasibility and the effectiveness of assimilating PR reflectivities. The case of tropical cyclone Zoe (December 2002) was investigated in detail. Results show a robust behavior of the 1D–Var with PR data. Its performance in terms of retrieved rainfall is comparable to that of other 1D–Var systems which make use of TRMM Microwave Imager (TMI) observations. When the 1D–Var TCWV pseudo–observations are input in the 4D–Var system, a positive impact is shown in the analysis and the subsequent forecasts both on moist–related fields and also on winds and surface pressure. The quality of the forecast is verified using track observations for the tropical cyclones. The track forecasts from the experiments which include the 1D–Var TCWV are generally closer to the observed track than a control run. Even if the number of TCWV values is substantially lower than that from the 1D–Var which uses TMI data due to the smaller spatial coverage, the PR data have an impact of comparable magnitude.

These results show that active sensor data can provide indirect yet useful information on the moisture field and that this information can effectively be assimilated to improve the analysis and the forecast of tropical disturbances.

1. Introduction

Precipitation retrievals/analyses are fundamental to understanding and improving the model description of the hydrological cycle. Numerical prediction models have improved considerably over the past few years in the analysis and the forecast of precipitation thanks to progress in both parameterizations and data assimilation. However, there is still the need to explore new avenues for model improvement through assimilation of data from active and passive sensors. In the near future, an increasing number of observations providing 3D information on clouds and precipitation will become available from spaceborne active instruments onboard various satellite platforms such as the Global Precipitation Mission, and its European component, EGPM; CloudSat; the Cloud–Aerosol Lidar and Infrared Pathfinder Satellite Observations; and the EARTH Cloud Aerosol Radiation Experiment. The challenge will be to maximize the amount of information that can be extracted from this data source and transformed through the model into knowledge about the atmospheric state.

Several authors have explored the impact of assimilation of precipitation data from various sources to improve analysis and forecast of both global and mesoscale models (e.g.,Zupanski et al. (2001), Zupanski et al. (2002), Zou and Kuo (1996), Tsuyuki (1997)). The feasibility of assimilating satellite–derived rainrates has also been demonstrated in a number of studies. Hou et al. (2000) show how assimilation of TMI rainfall rates and Total Precipitable Water (TPW) into a single column version of the Goddard Earth Observing System (GEOS) model improves diagnoses of clouds and radiation in areas of active convection and the distribution of latent heating in the Tropics, while reducing systematic errors in the forecasts. In a follow–up study,Hou et al. (2003) show that assimilation of TMI and SSM/I surface rainfall yields more realistic analysis of storm structures. Forecast skills are also improved as a result of the inclusion of rainfall information.

Since 1998, there has been an ongoing effort to assimilate satellite rainfall data into the ECMWF model. Marécal and Mahfouf (2000) initiated work toward that goal by using surface rain rates to correct the model first guess (background) in a one–dimensional variational context. Their results showed that the model first guess could be improved upon using the observations; however, when the same observations were used di-

rectly in the full ECMWF 4D–Var assimilation system, convergence to the optimal solution was not always attainable, because of the technical set–up of the operational incremental 4D–Var (inconsistencies between inner/outer loops, spectral/grid point representation of specific humidity, and possibly differences between nonlinear and simplified physics). To bypass this problem they resorted to a 1D+4D–Var approach in which the TMI surface rainrates are first processed with the 1D–Var system and the corresponding increments in specific humidity are then converted into pseudo–observations of Total Column Water Vapor (TCWV) that can be easily ingested in the 4D–Var system (Marécal and Mahfouf, 2002). This procedure has the advantage of ensuring better convergence and propagating the information coming from the rainy pixels to the dynamics by using a moisture–related variable. Their work has been continued and extended to the 1D–Var and 1D+4D–Var assimilation of brightness temperatures via the use of a radiative transfer operator and its adjoint byMoreau et al. (2003a, 2004). These authors show positive results from the quasi–operational TMI/SSMI 1D+4D–Var assimilation for a number of tropical cyclones and hurricanes. TCWV from rainy pixels is assimilated, when available, within the twelve–hour assimilation window providing some constraint on the time evolution of the storm. In most cases, the forecast of the cyclone track and the cyclone intensity is improved with respect to the control run when TMI or SSM/I observations are assimilated.

This study represents a complement to Moreau et al. (2004) and investigates the potential of the TRMM Precipitation Radar data. While PR data have been used for diagnostics and model evaluation, for the first time they are the direct subject of assimilation. The specific goals of this study are (i) to demonstrate that the 1D–Var system can handle the vertical information contained in the radar reflectivity and distribute it into significant temperature and humidity increments and (ii) to show that the impact of the Total Column Water Vapor increments derived from the PR reflectivities in the 4D–Var can be comparable to the impact from the assimilation of TMI–derived TCWV, despite the difference in spatial coverage between the two instruments, provided the PR samples “meaningful” portions of the storm.

The road map of the paper is as follows. Section **2.** briefly introduces the 1D+4D–Var technique used at ECMWF to assimilate rain information from the TMI and SSM/I measurements. This procedure is currently being adopted for the operational assimilation of brightness temperatures into the ECMWF model. Section **3.** presents the 1D–Var retrievals with PR data. A description of the observational operator used to derive radar reflectivities at 13.8 GHz from ECMWF three–dimensional model fields is also provided. Results from the 1D+4D–Var experiments are introduced and discussed in section **4.** A conceptual experiment using nadir–only data, which re–create the viewing geometry of the upcoming spaceborne radar mission CloudSat (Stephens et al., 2002), is described and discussed in section **5.** Finally, section **6.** provides a summary and draws some conclusions from this study.

2. Philosophy of the 1D+4D–Var approach

In the past years, a two–step strategy for assimilation of rain rates or rain–affected radiances has been developed at ECMWF. The first step is to perform a 1D–Var assimilation of the observed quantity using a simplified version of the model physics in which the aim is to adjust model variables such as temperature and specific humidity. The second step is the assimilation of the 1D–Var retrieval products into the 4D–Var system as pseudo–observations. This procedure was successfully applied at ECMWF for Television Infrared Observation Satellite (TIROS) Operational Vertical Sounder (TOVS) clear–sky radiances (Eyre et al., 1993) and for the SSM/I brightness temperatures in clear–sky areas (Gérard and Saunders, 1999). Marécal and Mahfouf (2002) applied this procedure to assimilate TMI rainfall retrievals and showed the feasibility of global assimilation of rain–related observations.

Ideally, direct 4D–Var assimilation would be more desirable because it allows for a better connection between

observations and model physics and avoids the introduction of correlations between model state and observations in the global system (linked to the double use of the background). However, the current ECWMF assimilation system is not tuned to assimilate observations of intermittent quantities such as rainfall, due to the incremental formulation. This computationally–efficient formulation of 4D–Var (Courtier et al., 1994) implies the calculation of the background trajectory and the observation departures (observation minus model) at high resolution using the full nonlinear model, and the iterative minimization of the cost function in a low–resolution space using the tangent linear model and its adjoint with simplified linearized physical parameterizations. For continuous fields, the different resolution between inner and outer loop does not affect negatively the results of the minimization. For highly nonlinear and inhomogeneous fields such as clouds and precipitation, this difference in resolution sometimes results in a lack of convergence. In their subsequent work,Marécal and Mahfouf (2003) list a series of further problems for direct 4D–Var of rain rates. Amongst those, the use of parameterizations with strong nonlinearities and thresholds; the underlying assumptions of the 4D–Var formulation: perfect model, use of global background errors, tuned for non–rainy situations, and Gaussian statistics for the errors. Other obstacles are forecast error estimates that presume cloud–free conditions and likely model bias in rainy situations. Despite these problems, research toward direct 4D–Var assimilation of cloud and rain is still ongoing, although the 1D+4D–Var approach seems to be more easily applicable and robust for the present time.

3. 1D–Var Retrievals using radar reflectivity

Given an atmospheric background state of temperature, specific humidity and surface pressure (x_b), and a forward model (H) that relates the model state (x) to a set of observations (y), it is possible to solve the inverse problem in a variational context and derive the atmospheric state for which the least–square distance between the observations and their model counterparts reaches its minimum. This is obtained by minimizing the following functional

$$J = \frac{1}{2}(\mathrm{x}-\mathrm{x}_b)^T\mathbf{B}^{-1}(\mathrm{x}-\mathrm{x}_b) + \frac{1}{2}(H(\mathrm{x})-\mathrm{y})^T\mathbf{R}^{-1}(H(\mathrm{x})-\mathrm{y}) \quad (1)$$

where **B** represents the background error covariance matrix and **R** the observation error covariance matrix which includes both instrumental errors and forward model errors. The operator H allows to go from model space to observational space and is defined according to the type of observations of interest. In this study, this operator consists of two moist physics schemes: large–scale condensation (Tompkins and Janisková, 2003, 2004) and convective parameterizations (Lopez and Moreau, 2004), plus the radar reflectivity model described in the next section.

a. Radar forward model

The radar backscattering cross-section derived from the radar return power can be related to the amount of solid precipitation (rain and snow) and the amount of cloud ice/water content that the radar signal encounters in its path. The forward modeling of this radar signal can be performed by assuming a size distribution of the scatterers and by computing their optical properties. The hydrometeor optical properties are computed assuming all particles are spherical and applying the Mie solution at the frequency of interest (13.8 GHz for the PR). Extinction and scattering cross–sections are computed as functions of temperature, and integrated by assuming a Marshall–Palmer distribution for the precipitation–sized particles (Marshall and Palmer, 1948) and a modified–gamma distribution for the cloud particles. The radar reflectivity factor is proportional to the integral of the backscattering cross–section over the size distribution. A variable commonly used to describe the radar return is the equivalent radar reflectivity, Z, which represents the radar reflectivity factor of an equivalent volume of spherical water droplets. When the target is an ice cloud, it is necessary to convert the reflectivity

factor into an equivalent reflectivity Z. This is done in the forward model by assuming a fixed density for the snow and cloud ice particles. In presence of intense precipitation, the radar signal at 13.8 GHz is attenuated. By computing the total optical depth and the path–integrated attenuation the attenuated profile of reflectivity can be recovered. In this study, however, the attenuation–corrected reflectivity product from the TRMM 2A25 algorithm (Iguchi et al., 2000) is used and hence the computation of the attenuation is not required, although the radar forward model has that capability. To speed up computational time all reflectivity values computed with this model are collected in a look–up table and classified according to the values of temperature and liquid/ice water contents, which are direct outputs of the ECMWF model. A bilinear interpolation is then applied to extract the reflectivity value corresponding to the given temperature and hydrometeor content. A special treatment of the melting layer (Bauer, 2001) is also included in the computation of the look–up table. The reflectivity values contained in the look–up table were verified against those derived from other forward models and those derived from simple Z–R relationship. Comparisons showed that the current forward model provides reflectivities within a few dBZs of those derived with other methods.

b. Set–up

The 1D–Var retrievals are run off-line using a standard set–up. The background temperature and specific humidity profiles are taken from a 12–hour forecast of the ECMWF model with T511 spectral truncation (corresponding to approximately 40 km) and 60 vertical levels. These profiles of temperature, T, and specific humidity, q, along with surface pressure, p_s, tendencies, and other surface quantities are used in the moist physics routines to compute cloud properties (cloud cover, ice and liquid–water contents) and precipitation fluxes. The radar observation operator is then applied to the model fields to obtain the equivalent reflectivity. The direct outputs of the 1D–Var are the optimal temperature and specific humidity profiles; from these variables it is possible to derive precipitation and cloud amounts by running again the physical schemes. The background error covariance matrix is taken from the operational ECMWF 4D–Var system (Rabier et al., 1998) (see Fig. 1 of Moreau et al. (2003b)). Temperature and specific humidity errors are assumed cross–uncorrelated.

c. TRMM/PR observations

A detailed overview of the specifications of the TRMM Precipitation Radar is presented in Kozu et al. (2001). Here only some general characteristics, that can be helpful to understand the type of rain/snowfall observations obtained with a spaceborne active sensor, are reported. The PR is a scanning radar which operates at 13.8 GHz; the cross–track scanning swath is 220 km and the cross–range spatial resolution is about 4.3 km at nadir. The vertical resolution is about 250 m. The minimum detectable signal is 0.7 mm h^{-1} which corresponds approximately to 17 dBZ when using Kozu et al.'s effective reflectivity–rainfall rate conversion ($Z = 372R^{5.4}$, Z in mm^6 m^{-3} and R in mm h^{-1}).

The PR data used in this study are the attenuation–corrected 13.8–GHz radar reflectivities from the standard TRMM 2A25 algorithm described in Iguchi et al. (2000). The attenuation correction is derived using a combination of surface echo and path integrated attenuation. Non–uniform beam–filling effects are also taken into account and corrected by assuming a probability distribution function for precipitation. The algorithm does not provide explicit error estimates for the whole reflectivity profile.

Since there is no automatic acquisition procedure for this TRMM product, at present the reflectivities are processed off–line for selected cases, averaged horizontally over the Gaussian grid of the model and interpolated vertically to model levels.

d. Assignment of uncertainties and data screening

A first approach to the error specification was to use a vertically–varying profile, based on the fact the accuracy of the reflectivity must increase with decreasing attenuation, i.e. with increasing altitude. The error profile was hence assigned as a linear function of height between 3 dBZ near the surface and 1 dBZ at 8 km. Above 8 km the error was assumed constant and equal to 1 dBZ. Since it was observed that no benefits were obtained from using this (arbitrary) error profile and since no scientific basis other than common sense could be invoked to support our choice of profile, it was decided to simplify the problem by assigning at all levels an uncertainty σ_{obs} of 25% to the PR reflectivity which corresponds approximately to 1.2 dBZ. The averaging and interpolation procedures also introduce a representativeness error in the reflectivity. Ideally this error should be included in the matrix **R**, but it is currently neglected due to difficulties in its estimate. The sensitivity to the error assumptions is briefly discussed in section e.

To prevent an undesired impact from surface echo contamination, data below 1.5 km are not used in the 1D–Var. Likewise isolated values of reflectivities are screened to prevent instabilities in the minimization. Reflectivities below 16 dBZ are not used due to the sensitivity threshold of the PR instrument. At the end of each minimization, the retrieved profiles is quality–controlled and rejected if the analysis minus observation departure exceeds $\pm 3\sigma_{obs}$. In this case, the retrieval is reset to the background.

e. 1D–Var Results

The 1D–Var retrieval was applied to one super–typhoon (Mitag, 5 March 2002) and to one tropical cyclone which occurred in 2002 (Zoe, 26 December 2002), as well as to twenty–one occurrences of tropical cyclones in 2003 and a squall line over land (5 August 2003). In all circumstances the 1D–Var (hereafter, 1D/PR–Z) achieved convergence and produced robust results in terms of reflectivity and corresponding precipitation. Results are only shown and discussed in detail for the well-documented case of tropical cyclone Zoe.

Figure 1 illustrates the performance of the 1D/PR–Z retrieval by comparing the background reflectivity to the observed reflectivity for cyclone Zoe over the PR swath. It clearly appears that the cyclone is not located in the same position in the background and in the observations causing a mismatch in the reflectivity field. Panel (c) shows that the retrieval was successful in adjusting the temperature and specific humidity profiles in such a way to increase the hydrometeor contents and hence the reflectivity, while effectively changing the precipitation patterns.

Figure 2 shows a comparison of near–surface rainfall rates retrieved from different data sources and using different 1D–Var set–ups. The background precipitation is shown in panel (a), while the reference rainfall from the PATER algorithm (Bauer and Schluessel, 1993; Bauer et al., 2001) and from the TRMM 2A25 algorithm are shown in panels (b) and (c) respectively. Panel (d) shows the rainfall retrieved with a 1D–Var where the PATER rainfall rates in (b) were used as observations (1D/TMI–RR). Panel (e) shows the rainfall retrieved with a 1D–Var where the 2A25 rainfall from (c) rates were used as observations (1D/PR–RR). Finally, panel (f) illustrates the results of the 1D–Var where TMI brightness temperatures where used as observations (1D/TMI–TB), and panel (g) is the output in terms of rain–fall rates from the 1D/PR–Z (the corresponding reflectivity field is shown in Fig. 1, panel (c)). All 1D–Var runs share the same background field.

Using the PATER rainfall rates as a reference for the 1D/TMI retrieval and the 2A25 rainfall rates as a reference for the 1D/PR–Z retrieval, the overall agreement of the different retrievals is striking and the differences between retrievals are smaller than the departures from the background. Focusing on the details, however, it appears that the 1D/PR–Z is slightly more effective than the 1D/PR–RR in modifying the rain–fall field, especially in the south–west corner of the storm and in the north–east portion. Note that the only difference between

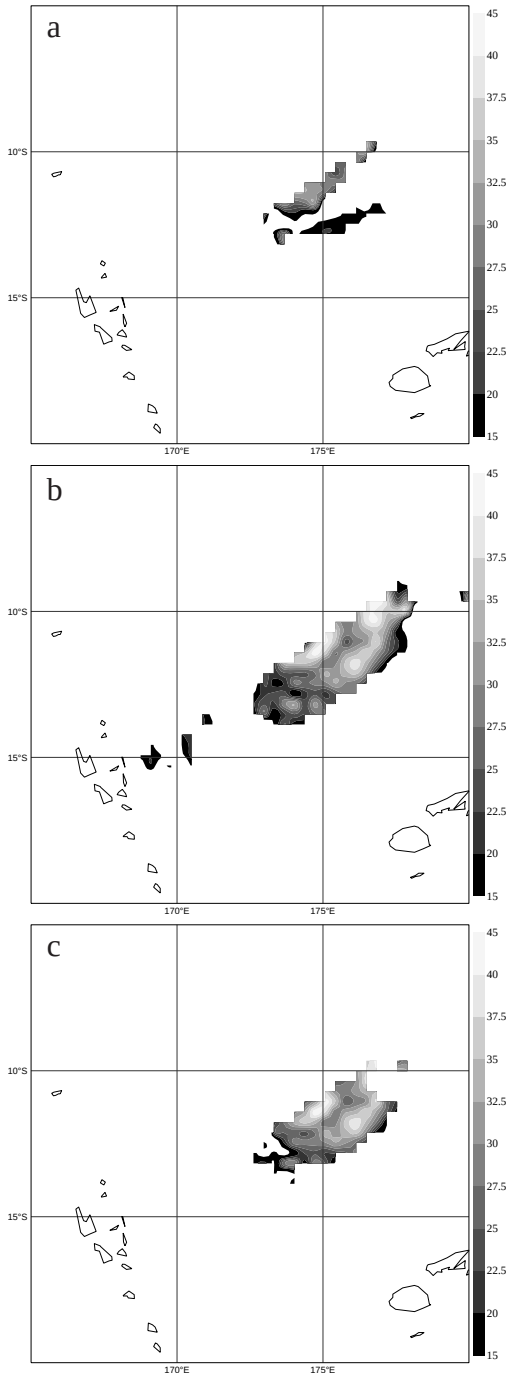

Figure 1: Near–surface unattenuated radar reflectivity (dBZ) for tropical cyclone Zoe at 1200 UTC 26 December 2002: (a) background field at 13.8 GHz; (b) 2A25 PR observations; and (c) output from the 1D–Var.

the two retrieval algorithms is the use of 2A25 attenuation–corrected reflectivities in the 1D/PR–Z versus the use of 2A25 rainfall profiles as observations. Similarly, in the 1D/TMI–TB the structure of the outer rain–band which extends south–west is better captured than in the 1D/TMI–RR. The 1D/TMI–RR and 1D/TMI–TB algorithm are extensively described and compared in Moreau et al. (2003b). Here, they are only used as sanity check for the performance of the 1D/PR–Z.

f. Sensitivity runs

The impact of the error assumptions on the 1D–Var results is assessed by comparing the reflectivity and the humidity increments from the standard run with 25% observation error at all levels and that from a run with 50% error at all levels. These are shown in panel (c) and (d) of Fig. 3 as vertical cross–sections between 13.5–9S and 173.5–178E. Panel (a) and (b) of the same figure show the background and the PR–observed reflectivities respectively. The effect of doubling the observational error is only evident in the bottom–right area of the plot, where the 1D/PR–Z gets less close to the observations due to the weaker constraint. However, in both configurations the 1D/PR–Z corrects the background and approaches the observations with realistic increments in specific humidity. The structure of this increments is similar in both cases with the exception of an area of negative increments indicating a decrease in specific humidity in the standard retrieval that is not present in the retrieval with double observation error.

A second impact study was performed to assess the benefits of using a full profile versus using a single–level observation. In panel (e) of Fig. 3, the reflectivity and humidity increments cross sections are shown for a run where only the 2A25 reflectivity at 2km was assimilated in the 1D/PR–Z. The error on this single–level reflectivity was fixed to 25% to compare the results with those from the standard run (panel c). As it appears from contrasting the two plots, the 1D/PR–Z with a single observation still manages to increase the reflectivity and to produce meaningful humidity increments in most points and gets closer to the observed cross section. However, further aloft a single–level observation does not have enough influence through vertical error correlations to substantially change the background field. When the retrieval is applied to a single–level observations, the 1D–Var relies heavily on the model and on the structure functions to distribute the increments in the vertical, hence the final temperature and humidity profiles are less reliable than those retrieved using the full profile of radar reflectivity.

These sensitivity runs support evidence of a good behavior of the 1D/PR–Z. The comparisons with other retrievals also offer an indirect proof of robustness of the 1D/PR–Z results.

4. 4D–Var experiments

In this section the results of the assimilation of 1D/PR–Z TCWV into the ECMWF model for selected cases studies are discussed. The specific humidity profiles analyzed with the 1D–Var were integrated vertically and the values of TCWV stored in an "observation" file along with its error estimate. This estimate stems naturally from the 1D–Var formulation. As shown by Rodgers (1976, 2000), the error on the retrieved variables can be expressed as a combination of the background error covariance matrix and the observation error covariance matrix weighted by the Jacobians as follows:

$$\mathbf{A} = [\mathbf{B}^{-1} + \mathbf{K}_n^T(\mathrm{x})\mathbf{R}^{-1}\mathbf{K}_n(\mathrm{x})]^{-1}, \tag{2}$$

where $\mathbf{K}_n(\mathrm{x}) = \left[\frac{\partial H(\mathrm{x})}{\partial \mathrm{x}}\right]_n$ represents the Jacobian matrix of the partial derivatives of the simulated reflectivity with respect to the control variable x and n is the index relative to the last iteration. In a perfectly linear

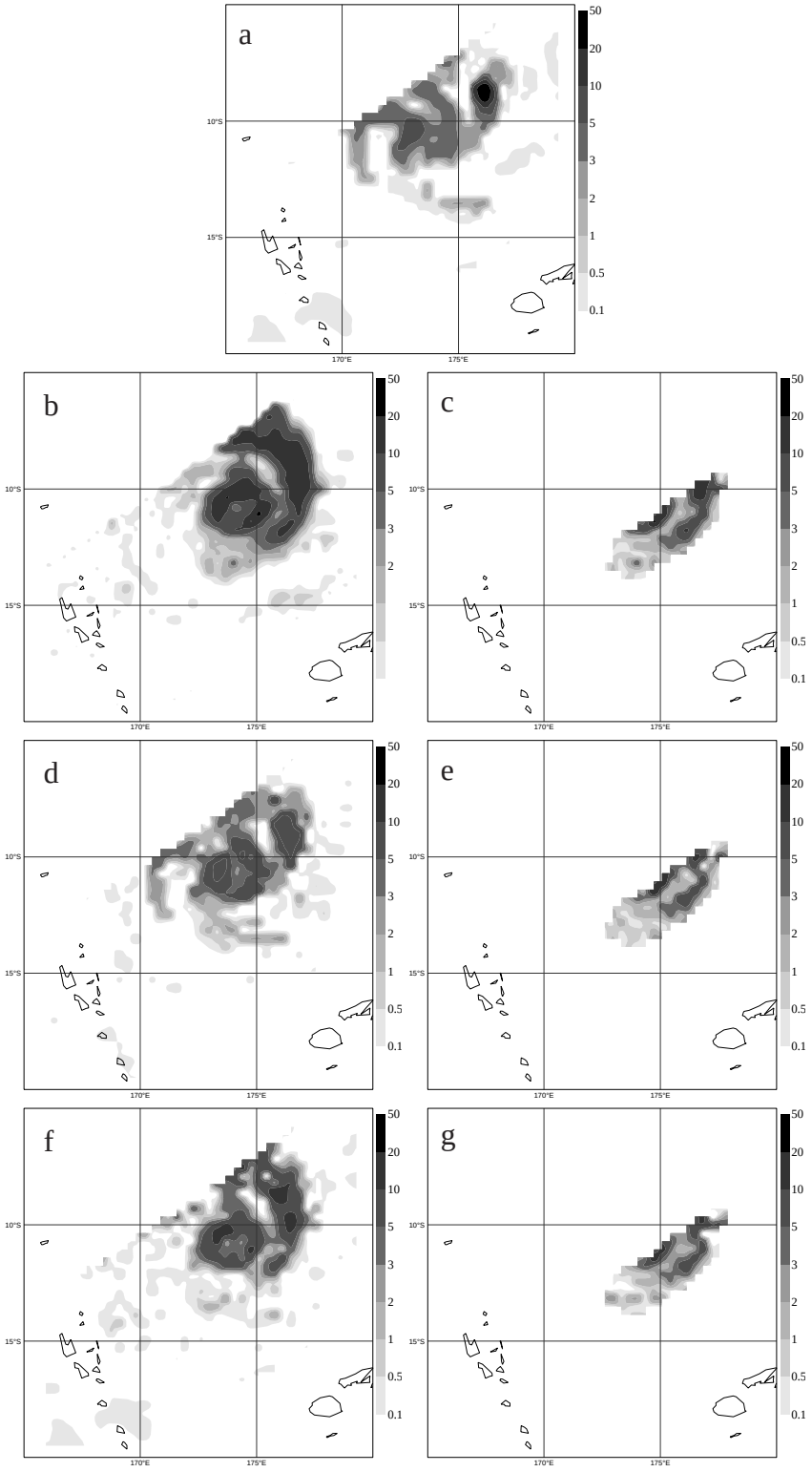

Figure 2: Near–surface rainfall rate (mm h^{-1}) for tropical cyclone Zoe at 1200 UTC 26 December 2002: (a) background field; (b) PATER product; (c) 2A25 product; (d) 1D/TMI–RR retrieval; (e) 1D/PR–RR retrieval; (f) 1D/TMI–TB retrieval; and (g) 1D/PR–Z retrieval. See text for explanations.

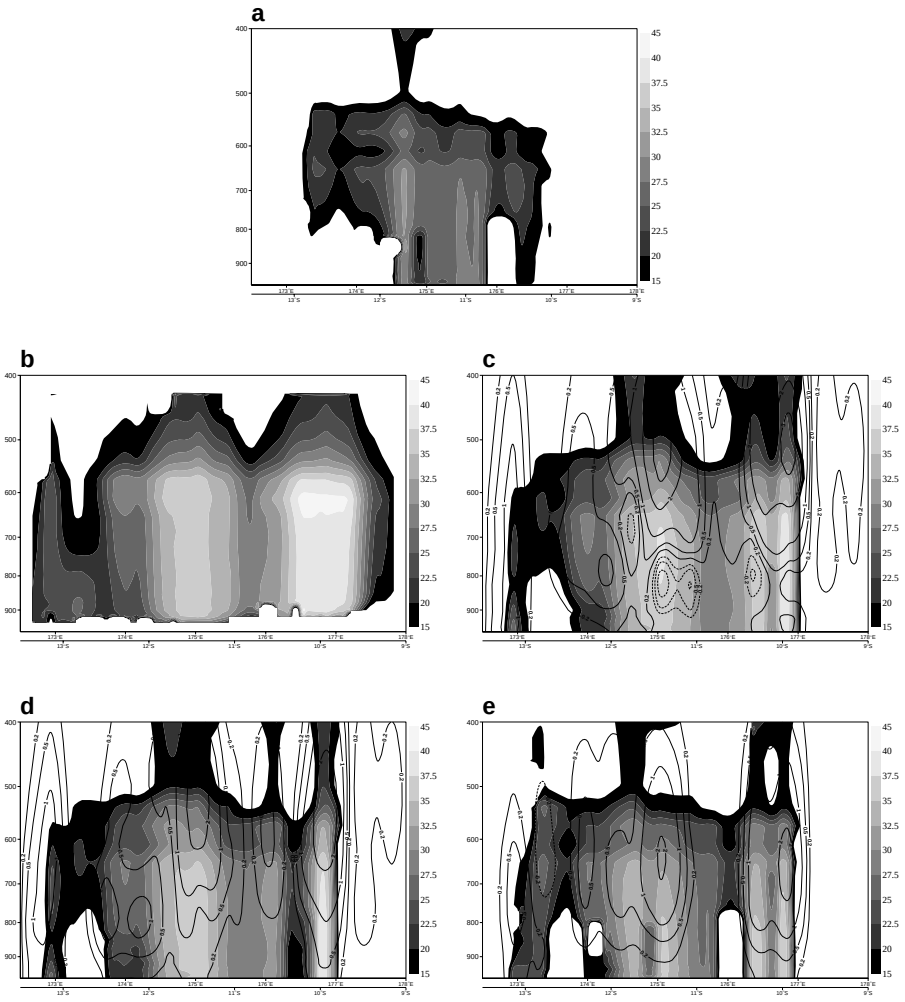

Figure 3: Vertical cross section of 13.8 GHz unattenuated radar reflectivity (shading, dBZ) and specific humidity increments (g/kg, positive increments in solid contours, negative increments in dashed contours) for tropical cyclone Zoe at 1200 UTC 26 December 2002: (a) background reflectivity; (b) 2A25 PR observations; (c) 1D–Var reflectivity all levels, 25% error on observations; (d) 1D–Var reflectivity all levels, 50% error on observations; and (e) 1D–Var reflectivity one level, 25% error on observation. See text for explanations.

problem, $\mathbf{K}(x)$ would not change from one iteration to the next since it would not depend on the new state. In the case of a non–linear observational operator, however, the Jacobians need be recalculated at every iteration. The error variance of the analyzed TCWV, σ_a, is then obtained by integrating the elements of the matrix **A** relative to specific humidity for every profile. To save computational time, Marécal and Mahfouf (2000) computed a fit to σ_a using a second–order polynomial function of the TCWV. In this study, we decided to use equation (2) which is deemed to be more accurate for the error calculation and not excessively expensive in the current 1D–Var parallel configuration. The values are on average comparable with those obtained with the Marécal and Mahfouf (2000) formulation.

a. Experiment set–up

A few of the 1D/PR–Z cases were selected to be tested in the 4D–Var. The configuration is the same for all experiments and uses the T511L60 ECMWF (40 km resolution, 60 vertical levels) model set–up (CY25R4) with 12 hour assimilation window. The 1D/PR–Z TCWV values available within three hours from the assimilation time (1200UTC or 000UTC, depending on the case) are all ingested at this time. Only one 4D–Var cycle is performed and a 10–day forecast is then run from the resulting analysis.

1D/PR–Z TCWV values are only assimilated in the proximity of the tropical cyclone in consideration. Hence, the number of TCWV pseudo-observations entering the 4D–Var is of the order of one hundred per case study. If compared with the number of points from a corresponding 1D/TMI–TB retrieval which is five times larger, the former appears negligible. One would expect almost no impact in the 4D–Var from the inclusion of this data. This is certainly true on a global scale, but if one focus on the forecast of a specific cyclonic event, then the effect of even few points can be significant, especially in data–void oceanic regions.

b. Results

The case of tropical cyclone Zoe is discussed in detail. For the other cases only the comparison of the track forecasts with observations is shown.

Figures 4–7 presents the comparison between a control run (hereafter, “control”) and an experiment in which the 1D/PR–Z TCWV pseudo–observations for cyclone Zoe were assimilated into the 4D–Var system (hereafter, simply “experiment”). To quantify the impact of these pseudo–observations, the following fields are analyzed: TCWV, temperature at 850 hPa, surface winds, mean sea level pressure (hereafter, MSLP), surface precipitation and surface convective precipitation. Figure 4 shows the TCWV differences between the experiment and the control at analysis time (1200UTC) and at forecast time +48h. The impact of the observations is evident in the analysis as well as in the 48h forecast, indicating that the TCWV increments are not “rained out” even if there is an increase in precipitation as shown in Fig. 6. Differences in TCWV can be as large as 10–15 kg m^{-2} and are mostly positive at the analysis time indicating a general moistening in the model as a direct consequence of the introduction of the 1D/PR–Z TCWV pseudo–observations. However the 48h forecast shows both areas of positive and negative increments, indicating a general redistribution in the atmospheric moisture. The temperature differences at analysis time are not as dramatic and do not exceed ± 3 K. However, these temperature changes can trigger precipitation formation in moist areas. The impact on the dynamical fields is small at the analysis time as shown in Fig. 5a. Since specific humidity errors contained in the **B** matrix are assumed to be univariate, the only way TCWV observations can influence the dynamical fields in the analysis is through the time integration over the twelve–hour 4D–Var assimilation window. In the forecast, in fact, the pressure field is largely modified in response to the different storm evolution as shown in Fig. 5b. The MSLP increments show a dipolar structure. In particular, an area of lower pressure (negative departures) is created on the east side of the storm, and a corresponding area of higher pressure (positive increments) is created on

the west side, indicating a shift in the storm position. This point will be further discussed when comparing the track forecast with observations. A similar impact is also seen in the wind field. Initially, there is little difference between the experiment and the control surface winds; as time goes by, however, the effect of the added moisture and the different precipitation pattern induces a dynamical response in the model such as to move the storm from its original location closer to the actual location as indicated by the PR observations.

Figure 6 shows the impact of the assimilation of 1D/PR–Z TCWV pseudo–observations on the precipitation field as differences between the near–surface rainfall in the experiment and in the control. The 12–hour forecast shows an overall increase in surface rainfall in excess of 10 mm h^{-1} mostly due to an increase in stratiform precipitation. Panels (b) and (c) of the same figure show the difference between the 24h minus the 12h forecast, and the 48h minus the 36h forecast. Both forecasts show higher values of precipitation in the experiment than in the control, and the difference is as pronounced as in the initial 12–hour forecast, although the location of the maximum has changed with the cyclone evolution. Panels (d) through (f) show the contribution to the precipitation differences deriving from the convection. For this cyclone, it appears that the main contributor to the total precipitation is the stratiform component, although the convective precipitation is higher in the experiment than in the control.

As further verification of the instantaneous precipitation in the forecast, the reflectivity derived from the experiment with the 1D/PR–Z TCWV pseudo–observations and that derived from the control were compared against TRMM/PR observations of tropical cyclone Zoe on December 28 at 400 UTC. These observations were not used in the assimilation and can be used to evaluate the two 40h forecasts started from the analyses at 1200UTC on December 26. We can see from Fig. 7 that the reflectivity field from the experiment is slightly closer to the PR observations particularly in the north–west and in the south–east part of the storm indicating a positive impact of the TCWV data on the medium–range forecast.

c. Track forecasts

An evaluation of the skills of the 4D–Var with 1D/PR–Z TCWV data is obtained by comparing the forecast track with observed track data (courtesy of the National Hurricane Center of the National Oceanic and Atmospheric Administration). The model tracking algorithm locates the cyclone by determining the position of the minimum MSLP and maximum vorticity via a recursive search mechanism (van der Grijn, 2002). Since the 4D–Var takes into account the temporal evolution of any variable within the assimilation window a modification of the humidity field due to the assimilation of the TCWV data will induce a dynamical response in the model. An initialization that takes into account the extra moisture or that has better knowledge of the position of the cyclone at the analysis time is expected to generate a better forecast of the cyclone itself in terms of both location and intensity.

Figure 8a shows a comparison of the observed track for tropical cyclone Zoe with the forecast track from the control run and from three 1D+4D–Var experiments where 1D/PR–Z, 1D/TMI–RR and 1D/TMI–TB data have been respectively assimilated in the analysis. The numbers correspond to forecast times. Besides considerations regarding forecast skills after 48 hours, which are beyond the scope of this paper, the assimilation of TCWV generally improves on the initial positioning of the cyclone and provides a better forecast of the location of the storm, confirming what observed in the structure of the MSLP increments (ref. Fig. 5). The experiment which provides the best track forecast is the 1D/TMI–TB. However, the 1D/PR–Z track is closer to the observations than the control run track and the improvement is comparable to that derived from the 1D/TMI–RR experiment. Considering the lower number of TCWV values that are ingested in the 1D/PR–Z 4D–Var experiment, this shows that PR data have a good potential for analysis and forecast improvement, at least for this case–study.

A comparison was also made between the track forecast resulting from the assimilation of the 1D/PR–Z TCWV

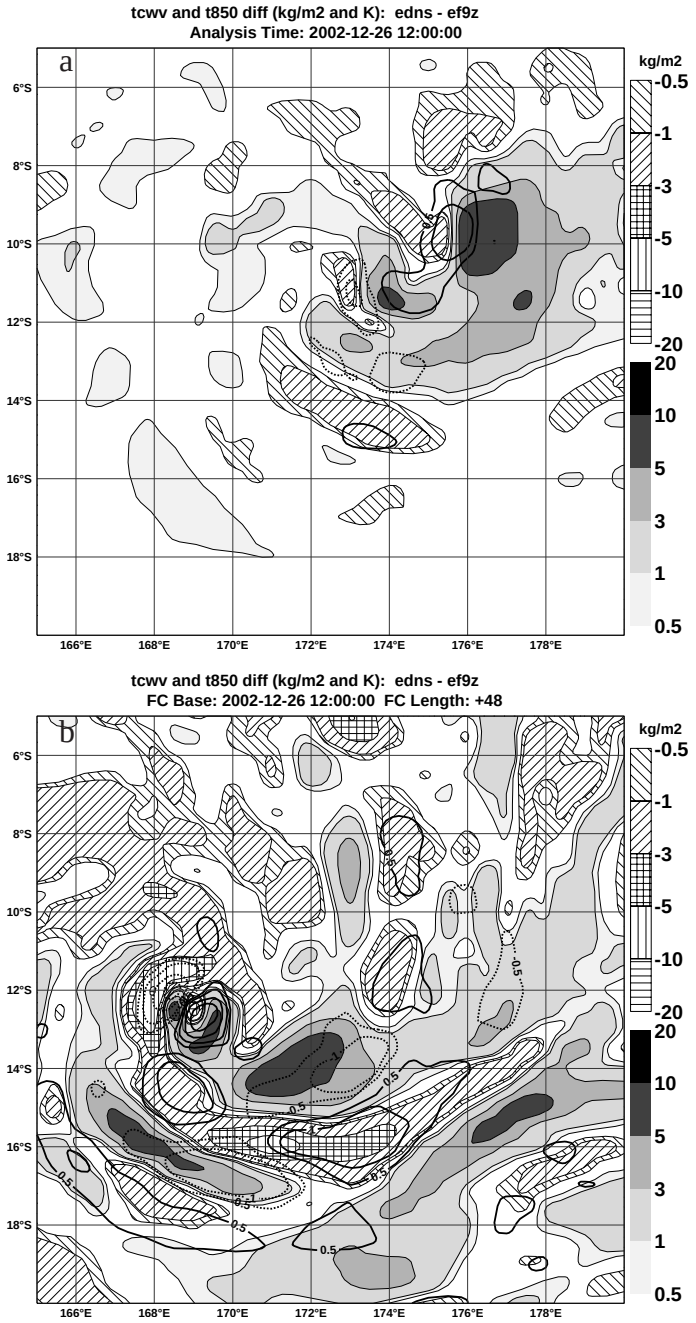

Figure 4: Differences between 4D–Var experiment and control run for cyclone Zoe on December 26, 2002. Total Column Water Vapour (kg m^{-2}, negative values in hatches and positive values in black–and–white shading) and Temperature at 850 hPa (K, positive increments in solid black contours and negative increments in dotted black countours): (a) analysis at 1200UTC using 1D/PR–Z TCWV pseudo–observations; and (b) 48h forecast.

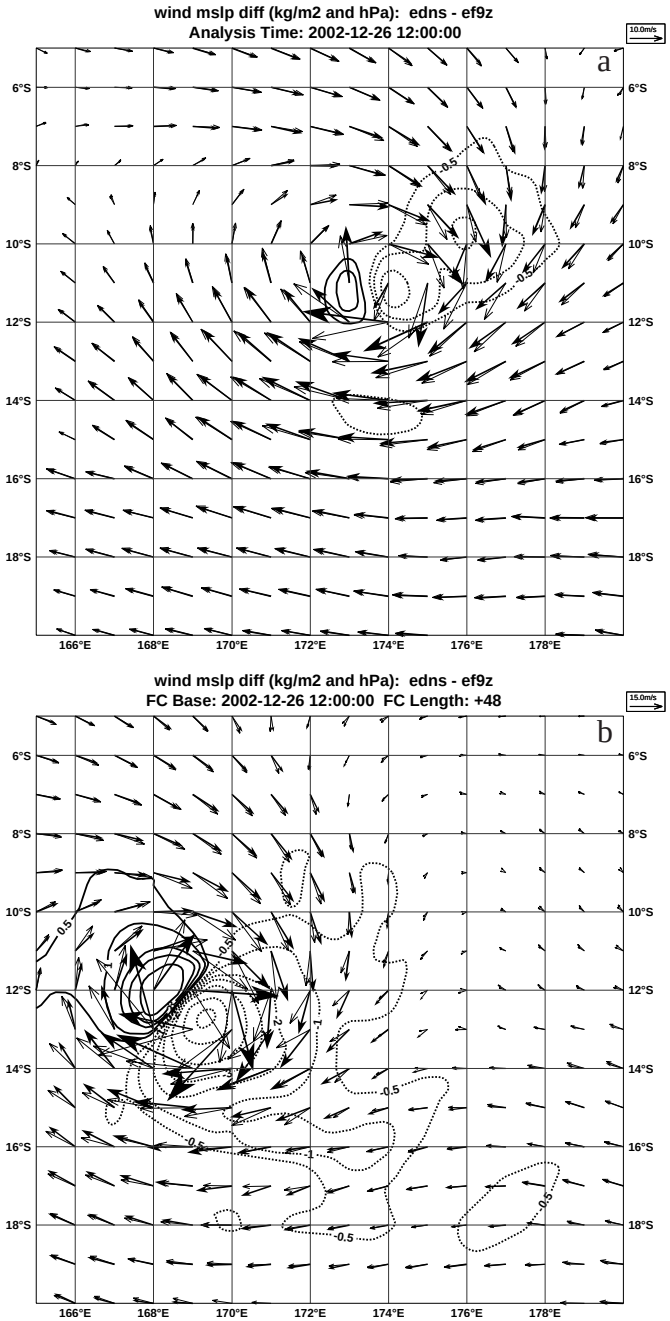

Figure 5: Differences between 4D–Var experiment and control run for cyclone Zoe on December 26, 2002. Wind field at 925 hPa (m/s, thin arrows for control and thick arrows for experiment) and the MSLP (hPa, positive increments in solid black contours and negative increments in dotted black countours): (a) analysis at 1200UTC using 1D/PR–Z TCWV pseudo–observations; and (b) 48h forecast. Wind vector units are 10 m/s in (a) and 15 m/s in (b).

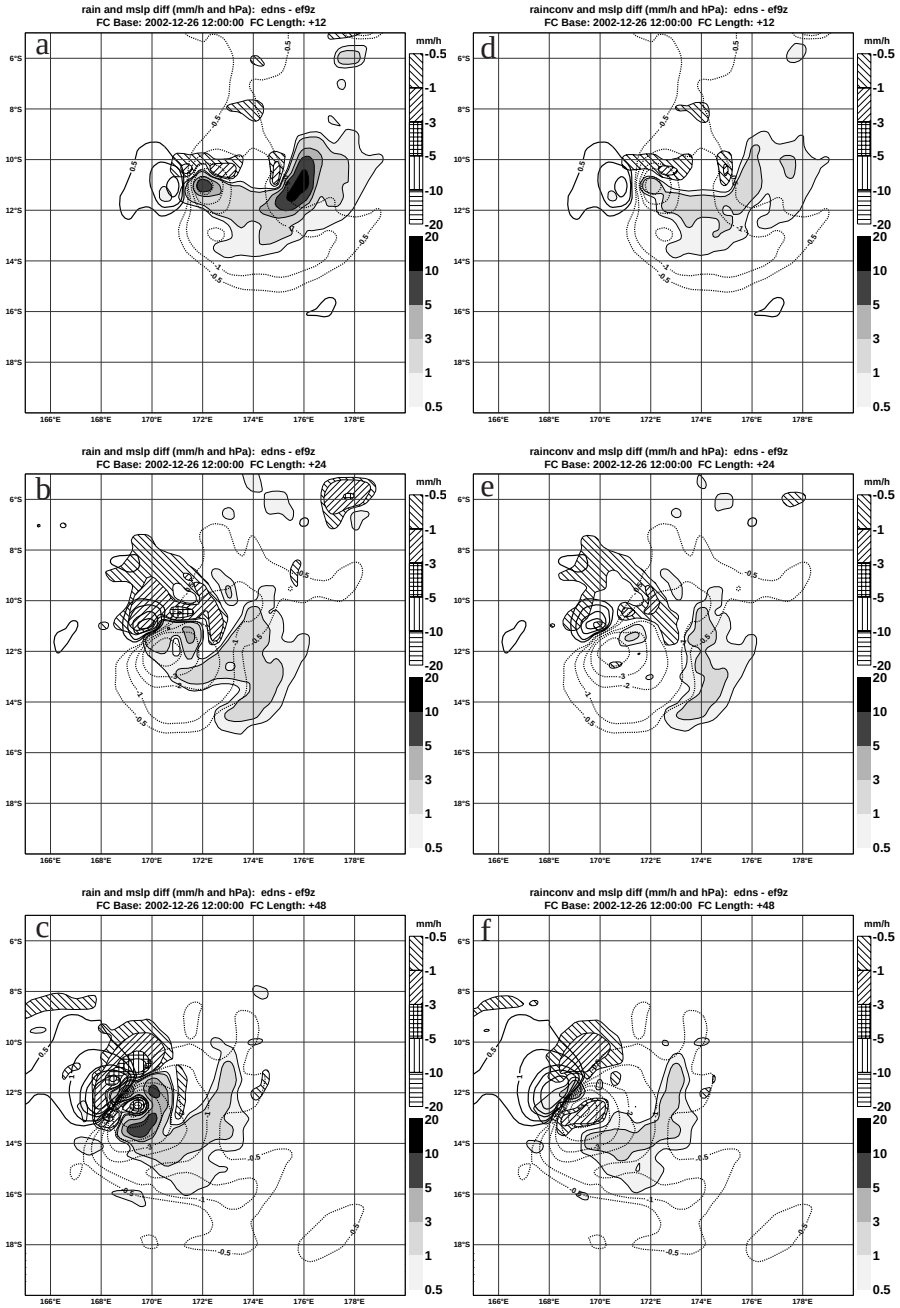

Figure 6: Differences between 4D–Var experiment and control run for cyclone Zoe on December 26, 2002. Left column shows total precipitation (mm h^{-1}, negative values in hatches and positive values in black–and–white shading): (a) 12h forecast from the analysis at 1200UTC; (b) 24h minus 12h forecast; and (c) 48h minus 36h forecast. Right column shows the convective precipitation (mm h^{-1}, negative values in hatched shading and positive values in black–and–white shading): (d) same as in (a); (e) same as in (b); and (f) same as in (c). MSLP is also shown for reference in all panels (hPa, black contours).

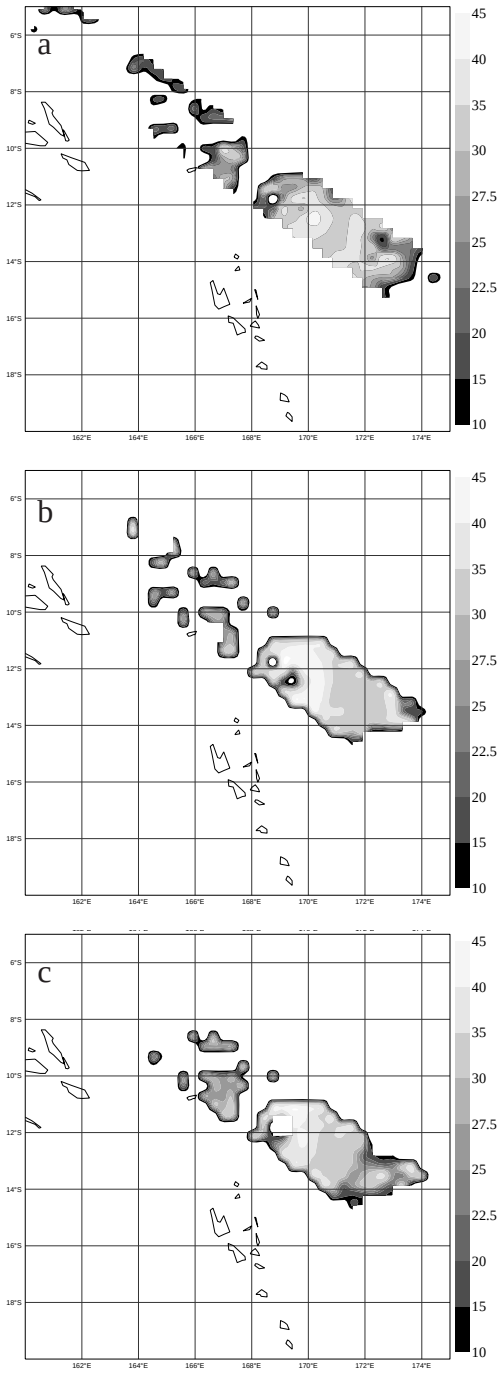

Figure 7: Near–surface unattenuated radar reflectivity (dBZ) for tropical cyclone Zoe at 400 UTC on 28 December 2002: (a) 2A25 PR observations; (b) 40h forecast started from the analysis on December 26 at 1200 UTC for the experiment with 1D/PR–Z TCWV pseudo–observations; and (c) 40h forecast started from the analysis on December 26 at 1200 UTC the control experiment.

and that from the assimilation of the 1D/PR–RR TCWV. Results shown in Fig. 9 indicate a slightly better performance of the experiment with 1D/PR–Z TCWV data, except between 12 and 24 hours.

Finally, Fig. 9 shows the comparison between the track forecast from a control run and the experiment with 1D/PR–Z TCWV data for tropical cyclones Gerry (55–80E/30–20S, February 13, 2003) and Kalunde (55–75E/25–15S, March 10, 2003). In both cases, despite the time lag between the forecasts and the observations (the cyclone in the forecast moves at a lower speed and there are differences in the trajectory), the run with the PR–derived TCWV produces tracks which are closer to the observed tracks.

d. Discussion of the 4D–Var results

The results from the 1D+4D–Var experiments prove that precipitation radar data contain information on moisture field which information can be extracted through a 1D–Var procedure and assimilated as TCWV pseudo–observations into the 4D–Var system to provide better initial conditions and better forecast of selected case studies. Results depend crucially on the PR sampling a core portion of the tropical cyclone and on the model providing initial background fields close to the observations. Limitations apply to cases in which the observation–background departures are so large that the increments implied by the 1D–Var, and hence the 1D/PR–Z TCWV observations, are too far removed from the background. In these cases the incremental system, which is based on the assumption of small departures from the model background trajectory, cannot handle the observations. This is a general prerequisite for the assimilation of any type of data and it is not specific to the PR reflectivities.

In three out of the four cases studied, the assimilation of 1D/PR–Z TCWV had a positive impact on the forecast of precipitation and storm location. The TCWV increments were also retained in the medium–range forecast thanks to the model propagating in time the information on the state variables derived from the observations and contained in the analysis.

5. CloudSat-type conceptual experiments

In this section an experiment that was carried out to show the potential of spaceborne active sensors which do not operate in a scanning configuration but rather have a fixed angle of viewing (generally nadir) is discussed. Although aware of the obvious differences between a precipitation radar and a cloud radar, to fix ideas it was useful to think of the CloudSat configuration with a nadir–looking radar sampling a small portion of the cyclone. The 2A25 PR reflectivities for cyclone Zoe were sampled and averaged only when the scanning angle was close to the nadir. With this screening the number of TCWV values available after the 1D/PR–Z was reduced from one hundred to eight points along the satellite track. One might think that this small number of points would have no impact on the cyclone forecast. However, since the TRMM overpass was sampling a meaningful portion of the cyclone, even with this reduced data–set it was possible to see a small positive impact after the assimilation of 1D/PR–Z TCWV.

To ensure that this result was not just coincidental, a second assimilation experiment was performed using opposite increments to those retrieved by the 1D/PR–Z to compute the pseudo–observations of TCWV. In other words, whenever the 1D/PR–Z had given a positive specific humidity increment with respect to the background, this was changed to a negative increment of the same magnitude with a resulting analyzed TCWV which was lower than the background (drying); viceversa for negative 1D/PR–Z specific humidity increments, the resulting analyzed TCWV was higher than the background (moistening). The rationale for this notional experiment was to show that as long as the pseudo–observations of TCWV are realistic, the 4D–Var analysis and forecasts are improved. However, if the TCWV values are prescribed to have opposite tendencies than what was retrieved, then the forecast resulting from the assimilation of such data becomes worse than both the control run and the

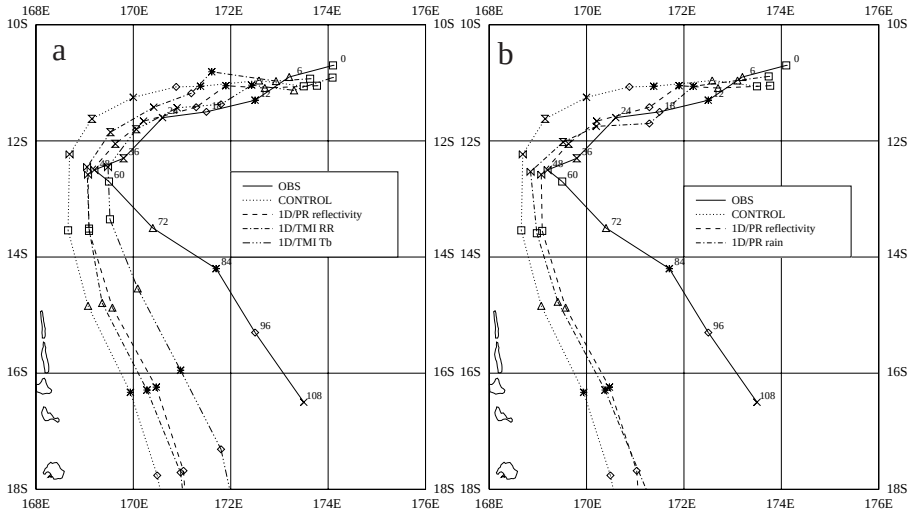

Figure 8: Comparison of forecast tracks with observed track of tropical cyclone Zoe on December 26, 2002: (a) observations (solid line), control run (dotted line), 1D+4D–Var assimilation with 1D/PR–Z TCWV (dashed line), 1D+4D–Var assimilation with 1D/TMI–RR TCWV (dash–dotted line), and 1D+4D–Var assimilation with 1D/TMI–TB TCWV (dash–three dotted line); (b) same as in (a) but for observations (solid line), control run (dotted line), 1D+4D–Var assimilation with 1D/PR–Z TCWV (dashed line) and 1D+4D–Var assimilation with 1D/PR–RR TCWV data (dash–dotted line). Numbers indicate forecast time in hours.

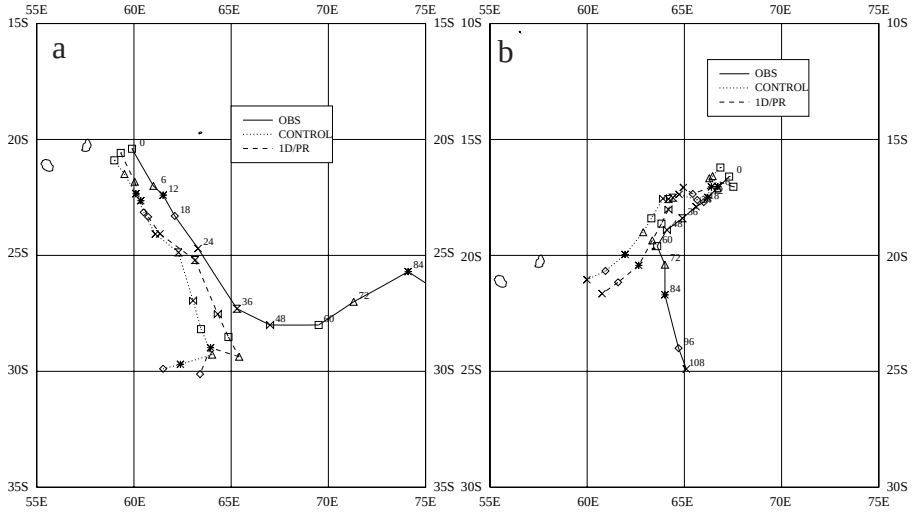

Figure 9: Comparison of forecast tracks with observed tracks. (a) Tropical cyclone Gerry (analysis time 1200UTC, February 13, 2003): observations (solid line), control run (dotted line), 1D+4D–Var assimilation with 1D/PR–Z TCWV (dashed line); and (b) same as (a) but for tropical cyclone Kalunde (analysis time 000UTC, March 10, 2003).

experiment with the “real” 1D/PR–Z TCWV data. Results from this conceptual experiment are shown in Fig. 10a. The experiment was partially successful in the sense that the track forecast resulting from the assimilation of the “real” 1D/PR–Z TCWV performs better than the control and the “false” 1D/PR–Z experiment in the first 48 hours. Afterwards, however it is the latter which produces a better track. At most short–term forecast times it is possible to see that the run with “false” 1D/PR–Z TCWV data is the furthest from the observed track whereas the opposite is true for the run with the “real” 1D/PR–Z TCWV data. The control run track places in between the two.

As a further verification of the hypothesis, the same conceptual experiment with tropical cyclone Gerry was repeated. Only nadir points (seven in total) were used in the assimilation. Results are shown in panel (b) of Fig. 10. It can be noticed that in this case the impact of the “real” 1D/PR–Z TCWV pseudo–observations is negligible, and actually slightly negative, at the beginning of the forecast. However, between 36 and 48 hours the forecast tracks from the 1D/PR–Z TCWV experiments is closer than the control run to the observed track. The forecast from the experiment with “false” 1D/PR–Z TCWV data has as well a negative impact at the beginning of the forecast and follows the operational forecast afterwards.

The main conclusion is that even a low number of observations in a data–void area can have a positive impact in the forecast of a specific case provided that the observations contain significant information relative to the meteorological situation of interest.

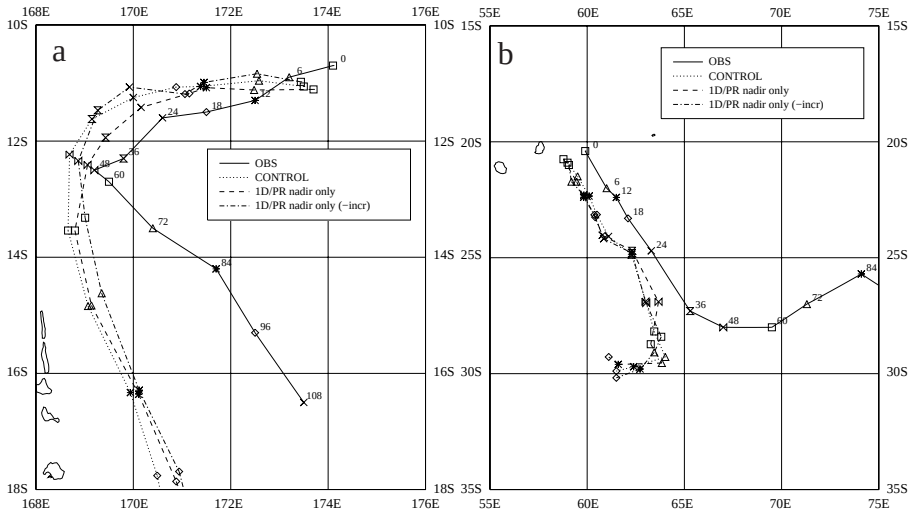

Figure 10: Comparison of forecast tracks with observed tracks. (a) Tropical cyclone Zoe (analysis time 1200UTC, December 26, 2002): observations (solid line), control run (dotted line), 1D+4D–Var assimilation with 1D/PR–Z TCWV (dashed line), 1D+4D–Var assimilation with 1D/PR–Z TCWV nadir–only with opposite increments (dash–dotted line); and (b) same as (a) but for tropical cyclone Gerry (analysis time 1200UTC, February 13, 2003). See text for explanations.

6. Summary and conclusions

This paper presented results from exploratory studies to assess the potential of reflectivity data from the Precipitation Radar onboard TRMM. This is the first time to our best knowledge that this type of data are used for assimilation. The approach to the assimilation follows that of Moreau et al. (2003b) and Marécal and Mahfouf (2002): a 1D–Var retrieval is first performed to retrieve temperature and specific humidity increments with

respect to the model first guess. Specific humidity increments are then vertically integrated to obtain Total Column Water Vapour values that can be introduced into the 4D–Var system as "pseudo–observations".

The results from the 1D/PR–Z were verified against other retrieval methods that share the same physical parameterizations but make use of different observational operators and use independent observations. The rainfall produced using 1D/PR–Z analyzed profiles of specific humidity and temperature compare well with both the PATER and the 2A25 products. Another point of strength of the 1D/PR–Z retrieval is that it can be applied over land, where most passive microwave retrievals suffer from uncertainties in the specification of the surface emissivity. Some sensitivity runs were performed to further evaluate the performance of the 1D/PR–Z. The use of a full vertical profile versus a single–level observation is beneficial in distributing the temperature and humidity increments to better match the observed reflectivity cross sections. The assumptions on the observational error, albeit important, do not affect the results dramatically. While research to better quantify both observation and forward model error is still ongoing, the 1D/PR–Z results appear to be robust to changes in the magnitude of those errors.

The impact of the assimilation of 1D/PR–Z TCWV data in 4D–Var is positive for most of the case studies that have been investigated. The increments in moisture at the analysis time are propagated to the forecast and converted into substantial changes of the dynamics. This is reflected in better track forecasts for the tropical cyclones under scrutiny when comparing the observed track to a control run and to the experiments where the 1D/PR–Z data were assimilated. Though limited in number, 1D/PR–Z TCWV data can be as effective as TCWV values derived from an instrument such TMI which samples a much wider swath.

Although 1D+4D–Var assimilation of radar reflectivities has so far been successfully tried on selected case studies, there is no obvious obstacle to experiment with a cycling of the analysis, mimicking the operational context, provided that model biases are quantified and corrected to ensure a correct behavior of the assimilation. To better exploit the vertical information deriving from the PR reflectivities, research is currently being done on how to include the full profiles of specific humidity and temperature retrieved by the 1D–Var into the 4D–Var system. Operational assimilation of satellite radar data could become a reality with the future missions (i.e., GPM) that will provide more frequent global measurements.

Acknowledgements

We would like to thank Jean–Noel Thépaut, Martin Miller and Anton Beljaars for suggestions and comments to improve the original manuscript. This research was performed under CloudSat NASA grant NAS5–99237 and European Space Agengy project EGPM (#3-10600/02/NL/GS).

References

Bauer, P.: 2001, Including a melting layer in microwave radiative transfer simulation for clouds. *Atmos. Research*, **57**, 9–30.

Bauer, P., P. Amayenc, C. D. Kummerow, and E. A. Smith: 2001, Over-ocean rainfall retrieval from multisensor data of the Tropical Rainfall Measuring Mission (TRMM). Part II: Algorithm implementation. *J. Ocean. Atmos. Tech.*, **18**, 1838–1855.

Bauer, P. and P. Schluessel: 1993, Rainfall, total water, ice water, and water vapor over sea from polarized microwave simulations and special sensor microwave/imager data. *J. Geophys. Res.*, **98**, 20737–20759.

Courtier, P., J.-N. Thépaut, and A. Hollingsworth: 1994, A strategy for operational implementation of 4d–var, using an incremental approach. *Q.J.R.Meteor.Soc.*, **120**, 1367–1387.

Eyre, J. R., G. A. Kelly, A. P. McNally, E. Andersson, and A. Persson: 1993, Assimilation of tovs radiance information through one–dimensional variational analysis. *Q. J. R. Meteorol. Soc.*, **119**, 1427–1463.

Gérard, E. and R. W. Saunders: 1999, Four–dimensional assimilation of Special Sensor Microwave/Imager total column water vapor in the ECMWF model. *Qyart. J. Roy. Meteor. Soc.*, **125**, 3077–3101.

Hou, A. Y., S. Q. Zhang, A. M. Da Silva, and W. Olson: 2000, Improving assimilated global datasets using TMI rainfall and columnar moisture observations. *J. Climate*, **13**, 4180–4195.

Hou, A. Y., S. Q. Zhang, and O. Reale: 2003, Variational continous assimilation of TMI and SSM/I rain rates: Impact on GEOS–3 hurricane analysis and forecast. *Mon. Weather Rev.*.

Iguchi, T., T. Kozu, R. Meneghini, J. Awaka, and K. Okamoto: 2000, Rain profiling algorithm for TRMM Precipitation Radar data. *J. Appl. Meteor.*, **39**, 2038–2052.

Kozu, T., T. Kawanishi, H. Kuroiwa, M. Kojima, K. Oikawa, H. Kumagai, K. Okamoto, M. Okumura, H. Nakatsuka, and K. K. Nishikawa: 2001, Development of Precipitation Radar onboard the Tropical Rainfall Measuring Mission (TRMM) satellite. *IEEE Trans. Geosci. Remote Sensing*, **39**, 102–116.

Lopez, P. and E. Moreau: 2004, A convection scheme for data assimilation: Description and initial tests. Technical report, ECMWF Technical Memorandum No. 411.

Marécal, V. and J.-F. Mahfouf: 2000, Variational retrieval of temperature and humidity profiles from TRMM precipitation data. *Mon. Weather Rev.*, **128**, 3853–3866.

— 2002, Four-dimensional variational assimilation of total column water vapour in rainy areas. *Mon. Weather Rev.*, **130**, 43–58.

— 2003, Experiments on 4d–var assimilation of rainfall data using an incremental formulation. *Q. J. R. Meteorol. Soc.*, **129**, 3137–3160.

Marshall, J. S. and W. M. Palmer: 1948, The distribution of raindrops with size. *J. Meteor.*, **5**, 165–166.

Moreau, E., P. Bauer, and F. Chevallier: 2003a, Variational retrieval of rain profiles from spaceborne passive microwave radiance observations. *J. Geophys. Res.*, **108**, dOI 10.1029/2002JD003315.

Moreau, E., P. Lopez, P. Bauer, A. M. Tompkins, M. Janisková, and F. Chevallier: 2003b, Variational retrieval of temperature and humidity profiles using rain rated versus microwave brightness temperatures. Technical report, ECMWF Technical Memorandum No. 412 (accepted for publication in *Q. J. Meteor. Soc.*).

— 2004, Variational retrieval of temperature and humidity profiles using rain rated versus microwave brightness temperatures. *Q. J. R. Meteorol. Soc.*, **130**, 827–852.

Rabier, F., A. McNally, E. Andersson, P. Courtier, P. Unden, J. Eyre, A. Hollingsworth, and F. Bouttier: 1998, The ECMWF implementation of the three dimensional variational assimilation (3D-Var). Part II: Structure functions. *Q. J. R. Meteorol. Soc.*, **124**, 1809–1829.

Rodgers, C. D.: 1976, Retrieval of atmospheric temperature and composition from remote measurements of thermal radiation. *Rev. Geophys. Space Phys.*, **14**, 609–624.

— 2000, *Inverse methods for atmospheric sounding*. World Scientific.

Stephens, G. L., D. G. Vane, R. Boain, G. G. Mace, K. Sassen, Z. Wang, A. J. Illingworth, E. J. O'Connor, W. Rossow, S. L. Durden, S. D. Miller, R. Austin, A. Benedetti, C. Mitrescu, and the CloudSat Science Team: 2002, The CloudSat mission and the A–train. *Bull. Amer. Meteor. Soc.*, **83**, 1771–1790.

Tompkins, A. M. and M. Janisková: 2003, A cloud scheme for data assimilation: Description and initial tests. Technical report, ECMWF Technical Memorandum No. 410.

— 2004, A cloud scheme for data assimilation: Description and initial tests. To appear in *Q. J. R. Meteorol. Soc.*

Tsuyuki, T.: 1997, Variational data assimilation in the tropics using precipitation data. part III: Assimilation of SSM/I precipitation rates. *Mon. Weather Rev.*, **125**, 1447–1464.

van der Grijn, G.: 2002, Tropical cyclone forecasting at ECMWF: new products and validation. Technical report, ECMWF Technical Memorandum No. 386.

Zou, X. and Y.-H. Kuo: 1996, Rainfall assimilation through an optimal control of initial and boundary conditions in a limited-area mesoscale model. *Mon. Wea. Rev.*, **124**, 2859–2882.

Zupanski, D., M. Zupanski, E. Rogers, D. F. Parrish, and G. J. Di Mego: 2001, Fine resolution 4DVAR data assimilation for the great plains tornado outbreak of May 3^{rd} 1999. *Wea. Forecasting*, **17**, 506–525.

Zupanski, M., D. Zupanski, D. F. Parrish, R. E., and G. J. Di Mego: 2002, Four–dimensional data assimilation for the blizzard of 2000. *Mon. Weather Rev.*, **130**, 1967–1988.